MALAYSIAN JOURNAL OF APPLIED SCIENCES 2024, VOL 9(2): 77-95
E-ISSN:0127-9246 (ONLINE)
http://dx.doi.org/10.37231/myjas.2024.9.2.401
https://journal.unisza.edu.my/myjas

ORIGINAL ARTICLE

On the Laplace Adomian Decomposition Method Numerical Analysis of the Vaccine's Effect on Measles

Folashade Abigail Alade[1]*, Peter Ayo Alabi[1], Uche Constance Ankeli[1], Sabiu Mubarak[1]

Department of Statistics, Federal Polytechnic Ede, Osun State, Nigeria.

*Corresponding author: folashadealade932@gmail.com

Received: 22/06/2024, Accepted: 31/10/2024, Available Online: 31/102024

Abstract

The Laplace Adomian Decomposition Method (LADM) offers a robust numerical framework for analyzing the effects of vaccination on the dynamics of measles transmission. This study employs LADM to solve the differential equations governing the spread of measles within a population, focusing on the impact of vaccination rates on disease prevalence. By decomposing the nonlinear terms of the governing equations into a series, the method facilitates an efficient and accurate approximation of the solution without requiring linearization or perturbation techniques. Through simulations, we explore various vaccination strategies and their efficacy in reducing measles outbreaks. Results illustrate that as vaccination rates increase, the infected population declines over time, while a decrease in vaccination rates leads to a notable rise in the susceptible population. Specifically, when vaccination rates drop from 0.2 to 0.12, the susceptible population increases significantly, causing a drastic decrease in the infected population. Furthermore, a gradual rise in vaccination rates from 0.03 to 0.12 over one month correlates with a marked reduction in infections, particularly when the waning rate is low (0.01), as more individuals become less likely to contract the disease. Conversely, a higher waning rate results in an increased infected population. This study contributes to the existing literature by showcasing LADM as a powerful tool for infectious disease modeling, providing insights into vaccination impacts on measles transmission dynamics and supporting evidence-based decision-making in public health interventions. The findings underscore the necessity of continuous vaccination efforts to achieve herd immunity and mitigate the risks associated with measles outbreaks.

Keywords: Measles, Basic Reproduction Number, Stability Analysis, Sensitivity Analysis, Laplace Adomian Decomposition Method.

Introduction

The measles is an epidemic disease that has spread rapidly over the world in the recent past, and nations of nations cannot stress the importance of this. We all want to comprehend how and what led us to this setting. A mathematical model is an explanation of a system that makes use of terms

related to mathematics and ideas. Mathematical modelling is the process which produces a mathematical model. These are working in engineering and natural science domains as well as in non-physical systems such as the social sciences. One of the nation's most frequent bacterial viral diseases, measles develops quickly—within 14 days—according to (Yoo et al., 2018). It is within human power to influence the environment it resides in. Humans interact with an assortment of creatures in everyday affairs (Adewale, 2022; Gans, 1998). Because these interactions are sometimes harmful or destructive to both humans and other beings, humanity has developed approaches, tools, and modern technologies to help lessen the threat (Kumar et al., 2022). Biological hazards are a constant in our environment, and we continually deal with new issues despite advancements in technology (Coovadia et al., 2019; Veklych et al., 2020).

A type of such threat is viruses. They are found in the air, soil, and water as well as on solid surfaces; they are invisible to the eyes of humans and are the cause of several diseases that kill millions of people every [6]. Most recently, the outbreak of a novel corona virus strain, SARS-COV-2, resulted in a pandemic that died more than 200 000 individuals between May 1, 2020, and its first case reported in Wuhan, China, in December 2019 (Gergonne, 2004; Journal, 2004). Additionally, an essential reproduction number serves as the stability-governing threshold i.e. $R_0 < 1$ and unstable if $R_0 > 1$ of the illness at balance by (Measles & Rubella Virus, 2015) is a well-known tool used to forecast the prevalence of a disease during its outbreak since it allows for tracking the disease's trajectory and rise or decline in the population (Singh et al., 2015; Griffin, 2016; Vynnycky et al., 2018). Exponentially robust or differently at a constancy of the region at free of illnesses equilibrium $(R_0 < 1 \; or \; R_0 > 1)$ in (Oh et al., 2022; Suwoyo et al., 2023; Berhe et al., 2020; Berkovich, 1964; James et al., 1979). We utilize analysis, prediction, and experimental behaviour research to battle these illusory enemies. Mathematical methods like as differentiation, integration, and computational procedures are employed to convert observed data into models for analysis and prediction in (Kulsoom et al., 2023). In order to provide predictions, these models are analyzed, using predetermined parameters and initial conditions, and then solved analytically or numerically. For large quantities consisting of individuals, such as the measles, mathematical compartmental models are employed.

The deterministic model assigns individuals of the population to each subgroup, which reflects a different stage of the epidemic in (Palumbo et al., 1992; Plans-Rubió, 2020; Wang et al., 2014). The results of the numerical simulation produced by the well-known Laplace Adomian decomposition method encourage the idea that treatments can help slow the disease's rapid spread and also play a positive and crucial role in encouraging further research and the carrying out of control measures.

Materials and Methods

Model Formulation

N (t) represents the overall population within study. The distinct populations that make up the population R (t) are the following: exposed population E (t), infected population I (t), vaccinated population V (t), and recovered population S (t). Considering this approach, the whole population is $N(t) = S(t) + V(t) + E(t) + I(t) + R(t)$. Population of the understudy is made up of birth rate θ, the point of contact with an infected individual is α, disease induced death rate of the measles

spread is δ An exposed individual can migrate to being infected at σ Vaccine waning rate on the immune of an infected is β_2 , rate of vaccination on vulnerable individual β_1, the recovery rate ρ and natural death on individual in the total population denoted by μ The above illustration can be represented in with schematic diagram and a system of nonlinear differential equations in figure 1 and equation 1 respectively.

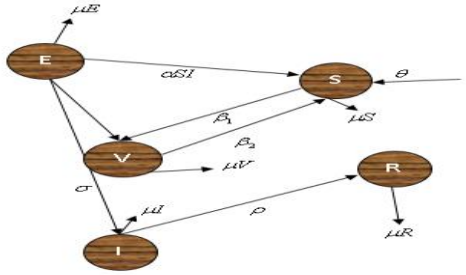

Figure 1. Flow of the model formulation

The system of the model formulated is presented as;

$$\left.\begin{aligned}
\frac{dS}{dt} &= \theta - \alpha SI - \beta_1 S + \beta_2 V - \mu S \\
\frac{dV}{dt} &= \beta_1 S - (\beta_2 + \mu)V \\
\frac{dE}{dt} &= \alpha SI - (\mu + \sigma)E \\
\frac{dI}{dt} &= \sigma E - (\mu + \delta + \rho)I \\
\frac{dR}{dt} &= \rho I - \mu R
\end{aligned}\right\} \qquad (1)$$

Subject to the following initial conditions

$$S(0) = s_0, V(0) = v_0, E(0) = e_0, I(0) = i_0, R(0) = r_0 \geq 0 \qquad (2)$$

Table 1. Description of parameters, values, and references

Variable	Description	Values	References
S(t)	Susceptible population	1200	1
V(t)	Vaccinated population	420	4
E(t)	Exposed population	68	7
I(t)	Infected population	27	11
R(t)	Recovered population	92	3
Parameter	**Description**	**Values**	**References**
ρ	Recovery rate	0.0375	4
σ	Migration rate from exposed to infected	0.0001	8
α	Disease contact parameter	0.2	Assumed
β_2	Vaccine waning rate	0.013	20

β_1	Vaccination rate of vulnerable	1.263	2
μ	Mortality rate	0.02	10
δ	Disease induced death	0.038	14
θ	Recruitment rate	1.29	Assumed

Analysis of the model

Positivity and Boundedness of Model Solution

The system (1), which describes an epidemic disease within a human population, should have parameters that are nonnegative. To ensure that the system of differential equations in (1) is both mathematically and epidemiologically well-posed, it is essential to demonstrate that the state variables in the model are nonnegative. System (1) is well-posed when the system starts with nonnegative initial conditions $S(0)=s_0, V(0)=v_0, E(0)=e_0, I(0)=i_0, R(0)$; In that case, the solutions of system (1) will persist in being nonnegative throughout their evolution, $t>0$ and that these positive solutions are bounded. We thus apply the following theorems.

Theorem 1

All solutions of system (1) are bounded.

Proof:

Consider the total population

$$N(t) = \mathrm{S(t)} + \mathrm{V(t)} + \mathrm{E(t)} + \mathrm{I(t)} + \mathrm{R(t)} \quad (3)$$

The variation in the total population concerning time is given by:

$$\frac{dN(t)}{dt} = \frac{d}{dt}\left(\mathrm{S(t)} + \mathrm{V(t)} + \mathrm{E(t)} + \mathrm{I(t)} + \mathrm{R(t)}\right) \quad (4)$$

Such that

$\frac{dN(t)}{dt} = \theta - \mu(S+V+E+I+R) - \delta I \quad \Rightarrow \frac{dN(t)}{dt} \le \theta - \mu N$ When no outbreak of measles, $\delta = 0$.Thus, it is obtained that

$\frac{dN(t)}{dt} + \mu N \le \theta$, leading to $N(t)e^{\mu t} = \frac{\theta}{\mu}e^{\mu t} + L$, L is the constant of integration (5)

Initially,

$N(0) = \frac{\theta}{\mu} + Le^{-\mu(0)}$, this yields

$$L = N(0) - \frac{\theta}{\mu} \quad (6)$$

Thus, substituting (6) into (5) as time progressively increases yields:

$$\lim_{t\to\infty} N(t) \le \lim_{t\to\infty}\left[\frac{\theta}{\mu} + \left(N(0) - \frac{\theta}{\mu}\right)e^{-\mu t}\right] = \frac{\theta}{\mu} \quad (7)$$

If so $N(0) \le \frac{\pi N}{\mu}$, as $N(t) \le \frac{\pi N}{\mu}$. This is a positive invariant set under the flow described by (2) so that no solution path leaves through any boundary $\Re_+^5$. However, it is sufficient to consider the dynamics of the model in the domain $\Re_+^5$. In this region the model can be considered has been mathematically and epidemiologically well-posed.

This shows that the total population $N(t)$, and the subpopulation $S(t), E(t), I(t), R(t)$ of the model are bounded and is a unique solution. Hence, its applicability to study physical systems is feasible.

Theorem 2

Given that the $S(0) = s_0 > 0, V(0) = v_0 > 0, E(0) = e_0 > 0, I(0) = i_0 > 0, R(0) = r_0 > 0$, and $\lambda > 0$, then the solutions $S(t), V(t), E(t), I(t), R(t)$ of the system (1) will always be nonnegative. Consider the compartment of the system of equations for case (1) on the population, as obtained.

Proof:

Let:

$$\Psi = \left\{ \left(S(t), V(t), E(t), I(t), R(t)\right) \in \Re_+^5 : N(t) \le \frac{\pi N}{\mu} \right\} \quad (8)$$

If $f_i, i = 1,2....5$ where f is a constant.

$$\begin{aligned} f_1 &= \theta - \alpha SI - \beta_1 S + \beta_2 V - \mu S \\ f_2 &= \beta_1 S - (\beta_2 + \mu)V \\ f_3 &= \alpha SI - (\mu + \sigma)E \quad , \quad (9) \\ f_4 &= \sigma E - (\mu + \delta + \rho)I \\ f_5 &= \rho I - \mu R \end{aligned}$$

Then,

$$\left.\begin{aligned} &\left|\frac{df_1}{dS}\right| = \left|(\alpha + \beta_1 + \mu)\right| < \infty, \left|\frac{df_1}{dV}\right| = \left|\beta_2\right| < \infty, \left|\frac{df_1}{dE}\right| = \left|0\right| < \infty, \left|\frac{df_1}{dI}\right| = \left|\alpha\right| < \infty, \left|\frac{df_1}{dR}\right| = \left|0\right| < \infty \\ &\left|\frac{df_2}{dS}\right| = \left|\beta_1\right| < \infty, \left|\frac{df_2}{dV}\right| = \left|(\beta_2 + \mu)\right| < \infty, \left|\frac{df_2}{dE}\right| = \left|0\right| < \infty, \left|\frac{df_2}{dI}\right| = \left|0\right| < \infty, \left|\frac{df_2}{dR}\right| = \left|0\right| < \infty \\ &\left|\frac{df_3}{dS}\right| = \left|\alpha\right| < \infty, \left|\frac{df_3}{dV}\right| = \left|0\right| < \infty, \left|\frac{df_3}{dE}\right| = \left|(\sigma + \mu)\right| < \infty, \left|\frac{df_3}{dI}\right| = \left|\alpha\right| < \infty, \left|\frac{df_3}{dR}\right| = \left|0\right| < \infty \\ &\left|\frac{df_4}{dS}\right| = \left|0\right| < \infty, \left|\frac{df_4}{dV}\right| = \left|0\right| < \infty, \left|\frac{df_4}{dE}\right| = \left|\sigma\right| < \infty, \left|\frac{df_4}{dI}\right| = \left|(\rho + \mu + \delta)\right| < \infty, \left|\frac{df_4}{dR}\right| = \left|0\right| < \infty \\ &\left|\frac{df_5}{dS}\right| = \left|0\right| < \infty, \left|\frac{df_5}{dV}\right| = \left|0\right| < \infty, \left|\frac{df_5}{dE}\right| = \left|0\right| < \infty, \left|\frac{df_5}{dI}\right| = \left|\rho\right| < \infty, \left|\frac{df_5}{dR}\right| = \left|\mu\right| < \infty \end{aligned}\right\} \quad (10)$$

Equation (7) demonstrates the presence of system (1) within the positive quadrant, leading it to ultimately enter and persist in the attracting subset Ψ. Consequently, the set comprises both the local and global attractors of system (1). As a result, the set is characterized as compact, positively invariant, and attractively influential with respect to the system. The solution of the model is bounded, well-posed and epidemiologically and mathematical represented.

Measles Non-Infected Equilibrium States

The measles-non-infected equilibrium state represents a scenario in which the system is entirely free from bacterial disease. Consequently, when the number of infected individuals (I), it follows that the numbers of exposed (E) and recovered (R), i.e. $I = E = R = 0$. In this context, the solution for the measles-free equilibrium point can be derived as follows:

$$\frac{dS}{dt} = \frac{dV}{dt} = \frac{dE}{dt} = \frac{dI}{dt} = \frac{dR}{dt} = 0 \qquad (11)$$

$$\begin{aligned} 0 &= \theta - \alpha SI - \beta_1 S + \beta_2 V - \mu S \\ 0 &= \beta_1 S - (\beta_2 + \mu)V \\ 0 &= \alpha SI - (\mu + \sigma)E \qquad (12) \\ 0 &= \sigma E - (\mu + \delta + \rho)I \\ 0 &= \rho I - \mu R \end{aligned}$$

At no outbreak of measles infection, the diseases class, at $t > 0$, from (12),

$\rho I - \mu R = 0$, $R = 0$. Similarly, $S = \dfrac{\theta(\beta_2 + \mu)}{\mu[\beta_1 + \beta_2 + \mu]}$ where $V = \dfrac{\theta\beta_1}{\mu[\beta_1 + \beta_2 + \mu]}$

Thus, the disease free equilibrium yields:

$$(S, V, E, I, R) = \left(S_0 = \frac{\theta(\beta_2 + \mu)}{\mu[\beta_1 + \beta_2 + \mu]}, V_0 = \frac{\theta\beta_1}{\mu[\beta_1 + \beta_2 + \mu]}, E_0 = 0, I_0 = 0, R_0 = 0 \right) \qquad (13)$$

Disease Steady State Prevalence

Measles prevalence on (S, V, E, I, R) at $t \neq 0$, highlighting its dynamic nature.to measure vital role on its outbreaks and protect the population. Let $E_e = (S^*, V^*, E^*, I^*, R^*)$ at steady state $I \neq 0$. Consider the system of equation in (1) the equilibrium points are:

$$\begin{aligned} S^\bullet &= \frac{(\mu + \sigma)(\mu + \delta + \rho)}{\alpha\sigma}, V^\bullet = \frac{\beta_1[(\mu + \sigma)(\mu + \delta + \rho)]}{\alpha\sigma}, \\ E^\bullet &= \frac{\theta\sigma\alpha + (\mu + \sigma)(\mu + \delta + \rho)[\beta_1\beta_2 - (\mu + \beta_1)]}{(\mu + \sigma)\alpha\sigma^2}, I^\bullet = \frac{\theta\sigma\alpha + (\mu + \sigma)(\mu + \delta + \rho)[\beta_1\beta_2 - (\mu + \beta_1)]}{(\mu + \sigma)(\mu + \delta + \rho)\alpha\sigma}, \qquad (14) \\ R^\bullet &= \frac{\rho(\theta\sigma\alpha + (\mu + \sigma)(\mu + \delta + \rho)[\beta_1\beta_2 - (\mu + \beta_1)])}{\mu(\mu + \sigma)(\mu + \delta + \rho)\alpha\sigma} \end{aligned}$$

Basic Reproduction Number

The basic reproduction number, denoted as R_0, measures the potential for measles infections. Only one of the two disease states has the potential to spread new infections. The model's

vulnerable and infectious compartments have connections by equation (1). This can also be referred to as the threshold parameter, that regulates the quick spread of an illness in a community, and it indicates the number of secondary infections brought on by those with the disease among the target group. To determine the system (1), we apply the next-generation method, focusing on the infectious classes E and I. This involves calculating the F and V matrices, representing the rates of new infections and transitions into and out of the infected compartment, respectively. From the equations in the system (1), we derive these matrices as follows. $R_0 = \rho(G - \lambda I|)$ where $G = F \times V^{-1}$ and ρ is the spectral radius of the matrix $|G - \lambda I|$.

From the system of equation (1) it is obtained for matrix F and V :

$$F_i = \left(\frac{\partial f_i(x_i)}{\partial x_j}\right), V_i = \left(\frac{\partial v_i(x_i)}{\partial x_j}\right) \quad (15)$$

Such that

$$f = \begin{pmatrix} \alpha SI \\ 0 \end{pmatrix},\ v = \begin{pmatrix} (\mu+\sigma)E \\ -\sigma E + (\mu+\delta+\rho)I \end{pmatrix} \quad (16)$$

Then,

$$F = \begin{pmatrix} 0 & \frac{\alpha\theta(\beta_2+\mu)}{\mu[\beta_1+\beta_2+\mu]} \\ 0 & 0 \end{pmatrix} V = \begin{pmatrix} (\mu+\sigma) & 0 \\ -\sigma & (\mu+\delta+\rho) \end{pmatrix}$$

$$V^{-1} = \begin{pmatrix} \frac{1}{(\mu+\sigma)} & \frac{\sigma}{(\mu+\sigma)(\mu+\delta+\rho)} \\ 0 & \frac{1}{(\mu+\delta+\rho)} \end{pmatrix} \quad (17)$$

Thus, the R_0 is obtained as

$$R_0 = \frac{\alpha\theta(\beta_2+\mu)}{\mu[\beta_1+\beta_2+\mu](\mu+\delta+\rho)} \quad (18)$$

Asymptotic Stability of Disease Free State

This section examines the stability of the disease-free state for measles by analysing the basic reproduction number's impact. When the reproduction number is $R_0 < 1$, the disease declines, and we determine stability using a Jacobian matrix and a characteristic equation.

Theorem 3

The disease-free state of the model is locally asymptotically Stable $R_o < 1$ and unstable if $R_o > 1$.

Proof:

The disease-free equilibrium is obtained as the Jacobian matrix of the system of (1) is obtained and evaluated at the disease free-state using the linearization method

$$J_{(E_1)}=\begin{pmatrix} -(\beta_1+\mu) & \beta_2 & 0 & -\alpha & 0 \\ \beta_1 & -(\beta_2+\mu) & 0 & 0 & 0 \\ 0 & 0 & -(\sigma+\mu) & 0 & 0 \\ 0 & 0 & \sigma & -(\mu+\delta+\rho) & 0 \\ 0 & 0 & 0 & \rho & -\mu \end{pmatrix} \quad (19)$$

Computing for the eigenvalues, $\left|J_{E_1}-\lambda_i I\right|=0$

$$\begin{vmatrix} -(\beta_1+\mu)-\lambda & \beta_2 & 0 & -\alpha & 0 \\ \beta_1 & -(\beta_2+\mu)-\lambda & 0 & 0 & 0 \\ 0 & 0 & -(\sigma+\mu)-\lambda & 0 & 0 \\ 0 & 0 & \sigma & -(\mu+\delta+\rho)-\lambda & 0 \\ 0 & 0 & 0 & \rho & -\mu-\lambda \end{vmatrix}=0 \quad (26)$$

as obtained:

$$\lambda=-(\beta_1+\mu),-(\beta_2+\mu),-(\sigma+\mu),-(\mu+\delta+\rho),-\mu \quad (20)$$

The eigenvalues are negatively invariant in the region $\Re_+^5$, hence the system of (1) is asymptotically stable.

Regional Resilience of the Persistence Equilibrium State

Theorem 4

The regional resilience of the persistent equilibrium of the proposed model is locally asymptotically Stable if and unstable otherwise.

Proof:

Suppose, $S=x+S^*, V=y+V^*, E=z+E^*, I=a+I^*, R=b+R^*$

Linearizing equation (1), is then obtained as

$$\left.\begin{aligned} \frac{dx}{dt}&=\theta-\alpha(x+S^*)(a+I^*)-\beta_1(x+S^*)+\beta_2(y+V^*)-\mu(x+S^*) \\ \frac{dy}{dt}&=\beta_1(x+S^*)-(\beta_2+\mu)(y+V^*) \\ \frac{dz}{dt}&=\alpha(x+S^*)(a+I^*)-(\mu+\sigma)(z+E^*) \\ \frac{da}{dt}&=\sigma(z+E^*)-(\mu+\delta+\rho)(a+I^*) \\ \frac{db}{dt}&=\rho(a+I^*)-\mu(b+R^*) \end{aligned}\right\}$$

$$\left.\begin{aligned}
\frac{dx}{dt} &= -\alpha x a - \beta_1 x + \beta_2 y - \mu x + \text{higher order} + \text{nonlinear terms...} \\
\frac{dy}{dt} &= \beta_1 x - (\beta_2 + \mu) y + \text{higher order} + \text{nonlinear terms...} \\
\frac{dz}{dt} &= \alpha x a - (\mu + \sigma) z + \text{higher order} + \text{nonlinear terms...} \\
\frac{da}{dt} &= \sigma z - (\mu + \delta + \rho) a + \text{higher order} + \text{nonlinear terms...} \\
\frac{db}{dt} &= \rho a - \mu b + \text{Higher order} + \text{nonlinear terms...}
\end{aligned}\right\} \quad (21)$$

Jacobian matrix of the system of (21),

$$J_{E^*} = \begin{bmatrix}
-(\alpha a + \beta_1 + \mu) & \beta_2 & 0 & -\alpha x & 0 \\
\beta_1 & -(\beta_2 + \mu) & 0 & 0 & 0 \\
\alpha a & 0 & -(\mu + \sigma) & 0 & 0 \\
0 & 0 & \sigma & -(\mu + \delta + \rho) & 0 \\
0 & 0 & 0 & \rho & -\mu
\end{bmatrix}$$

$$\begin{vmatrix}
-(\alpha a + \beta_1 + \mu) - \lambda & \beta_2 & 0 & -\alpha x & 0 \\
\beta_1 & -(\beta_2 + \mu) - \lambda & 0 & 0 & 0 \\
\alpha a & 0 & -(\mu + \sigma) - \lambda & 0 & 0 \\
0 & 0 & \sigma & -(\mu + \delta + \rho) - \lambda & 0 \\
0 & 0 & 0 & \rho & -\mu - \lambda
\end{vmatrix} = 0 \quad (22)$$

The resulting eigenvalue of the above matrix is obtained as;

$$-(\alpha a + \beta_1 + \mu) - \lambda, -(\beta_2 + \mu) - \lambda, -(\mu + \sigma) - \lambda, -(\mu + \delta + \rho) - \lambda, -\mu - \lambda = 0\} \quad (23)$$

If $p = -(\alpha a + \beta_1 + \mu), q = -(\beta_2 + \mu), r = -(\mu + \sigma), s = -(\mu + \delta + \rho), t = -\mu$ it's therefore obtained that

$$(p - \lambda)(q - \lambda)(r - \lambda)(s - \lambda)(t - \lambda) = 0$$

Algebraically, it is obtained that,

$$\lambda^5 - \big(t + (r + s) + (p + q)\big)\lambda^4 + \big((p + q)(r + s) + pq + rs\big)(1 + t)\lambda^3 - \big(pq(r + s) + rs(p + q)\big)(1 + s)\lambda^2 + s\big(pq(r + s) + rs(p + q)\big)\lambda - pqrst = 0$$

.

With the invariance of the Eigen values it is said to be locally asymptotically stable

Global Stability of the Disease Free

The global asymptotic stability of the disease-free equilibrium of the proposed model is demonstrated using the Lyapunov technique. This entails examining the equilibrium's time derivatives to show how the system eventually approaches a stable state. The description that follows lays out the steps involved in reaching this stability.

$$\Phi(t, S, V, E, I, R) = C_1 I_1 + C_2 I_2 \quad (24)$$

$$\frac{dV}{dt} = C_1 I_1^{\bullet} + C_2 I_2^{\bullet}$$
$$= C_1\left[\alpha S I_2 - (\mu+\sigma) I_1\right] + C_2\left[\sigma I_1 - (\mu+\delta+\rho) I_2\right]$$
$$= C_1 \alpha S I_2 - C_1(\mu+\sigma) I_1 + C_2 \sigma I_1 - C_2(\mu+\delta+\rho) I_2$$
$$\leq \left[C_2\sigma - C_1(\mu+\sigma)\right] I_1 + \left[C_1 \alpha S - C_2(\mu+\delta+\rho)\right] I_2$$
$$\frac{dV}{dt} \leq \left[C_2\sigma - C_1(\mu+\sigma)\right] I_1 + \left[C_1 \frac{\alpha\theta(\beta_2+\mu)}{\mu[\beta_1+\beta_2+\mu]} - C_2(\mu+\delta+\rho)\right] I_2 \leq N, S$$

If $C_1 = \frac{1}{(\mu+\sigma)}, C_2 = \frac{\alpha\theta(\beta_2+\mu)}{\mu[\beta_1+\beta_2+\mu](\mu+\sigma)(\mu+\delta+\rho)}$

$$\frac{dV}{dt} \leq \left[\frac{\sigma\alpha\theta(\beta_2+\mu)}{\mu[\beta_1+\beta_2+\mu](\mu+\sigma)(\mu+\delta+\rho)} - \frac{(\mu+\sigma)}{(\mu+\sigma)}\right] I + \left[\frac{\beta(1-c)\Lambda}{\mu(\mu+\varepsilon+\tau_1)} - \frac{\Lambda(1-c)\beta(\mu+\gamma+d+\tau_2)}{\mu(\mu+\varepsilon+\tau_1)(\mu+\gamma+d+\tau_2)}\right] I$$
$$\frac{dV}{dt} \leq \eta\left[\frac{\alpha\theta(\beta_2+\mu)}{\mu[\beta_1+\beta_2+\mu](\mu+\delta+\rho)} - 1\right] I$$
$$\frac{dV}{dt} \leq \eta(R_0 - 1) \qquad (25)$$

Imperatively to note that $\frac{dV}{dt} = 0$ only when $I = 0$, the substitution of $I = 0$ into the model system of equation (1) shows that $S_O = \frac{\theta(\beta_2+\mu)}{\mu[\beta_1+\beta_2+\mu]}$ as $\eta = \frac{\sigma}{(\mu+\sigma)}$ at $t \to \infty$. Based on LaSalle's invariance principle. Hence $I = 0$ is globally asymptotically stable whenever R_o > 1.

Sensitivity Analysis of the Basic Reproduction Number

The sensitivity of [the model or system] is evaluated concerning each parameter. The normalized forward sensitivity index, defined below, measures the impact of parameter variations on model outcomes. This index quantifies the relative importance of individual parameters in influencing the behaviour of the system under consideration. This analysis will result in the determination of the normalized forward sensitivity index, denoted as

$$\frac{\partial R_o}{\partial \rho} \times \frac{\rho}{\partial R_o} = \frac{\rho(\mu+\delta+\rho)}{(\mu+\delta)} = 0.01576632\ ,\ \frac{\partial R_o}{\partial \theta} \times \frac{\theta}{\partial R_o} = 1.00000$$
$$\frac{\partial R_o}{\partial \alpha} \times \frac{\alpha}{\partial R_o} = 1.00000,\ \frac{\partial R_o}{\partial \beta_1} \times \frac{\beta_1}{\partial R_o} = \frac{\beta_1[\beta_1+\beta_2+\mu]}{(\beta_2+\mu)} = 2.3070$$
$$\frac{\partial R_o}{\partial \beta_2} \times \frac{\beta_2}{\partial R_o} = \frac{\mu\beta_2[\beta_1+\beta_2+\mu]}{(\beta_1+\mu)(\beta_2+\mu)} = 1.2992\ ,\ \frac{\partial R_o}{\partial \mu} \times \frac{\mu}{\partial R_o} = \frac{\beta_2\mu^2[\beta_1+\beta_2+\mu](\mu+\delta+\rho)}{(\beta_1+\beta_2)(\beta_2+\mu)(\delta+\rho)} = -1.020123 \qquad (26)$$
$$\frac{\partial R_o}{\partial \delta} \times \frac{\delta}{\partial R_o} = \frac{\delta(\mu+\delta+\rho)}{(\mu+\rho)} = 0.0207777$$

Table 1. Sensitivity analysis and parameter indices

Parameters	Sensitivity indices
ρ	$0.01576632 \times days^{-1}$
β_1	$2.3070\, e^{-3} \times days^{-1}$
θ	$1.0000000 \times days^{-1}$
α	$1.0000000 \times days^{-1}$
β_2	$1.29925 e^{3} \times days^{-1}$
δ	$0.0207777 \times days^{-1}$
μ	$-1.020123 \times days^{-1}$

Table 2 shows that the sensitivity indices of are positive, the sensitivity indices depend on the values of the other parameters, and changes in those values will affect the sensitivity indices. Based on the table, we can conclude that parameters are the most sensitive to the basic reproduction number in equation (1) of the measles infection. Particularly, increasing the value of β_1 will result in 88.14% increase in R_o, while increasing the value of ρ will lead to a 1.67% increase in R_o.

Numerical Simulation

To conduct numerical simulation on the mathematical model, we create the following iterative scheme of Laplace adomian decomposition method for the model equation. The Laplace Adomian Decomposition method was employed to computationally analyse the epidemic model. Maple software facilitated the generation of iteration formulas for each compartment. These formulas were then iteratively solved, enabling the numerical evaluation of the model's dynamics and providing insights into the epidemic's behaviour and progression. Taking the Laplace transform of both sides of the above equation.

$$\left.\begin{aligned}
L\left[\frac{dS}{dt}\right] &= L[\theta] - L[\alpha SI - \beta_1 S + \beta_2 V - \mu S]L \\
L\left[\frac{dV}{dt}\right] &= L[\beta_1 S] - L[(\beta_2 + \mu)V] \\
L\left[\frac{dE}{dt}\right] &= L[\alpha SI] - L[(\mu + \sigma)E] \\
L\left[\frac{dI}{dt}\right] &= L[\sigma E] - L[(\mu + \delta + \rho)] \\
L\left[\frac{dR}{dt}\right] &= L[\rho I] - L[\mu R]
\end{aligned}\right\} \quad (27)$$

Following the definition of Laplace Transform of derivatives

$$L\left[f^{\bullet}(t)\right] = mf(t) - f(0) \qquad (3),$$

Substituting into (2) to yield

$$\left.\begin{aligned} mL[S(t)] &= S(0) + \frac{\theta}{m} + L[-\alpha[SI] - \beta_1 S + \beta_2 V - \mu S] \\ mL[V(t)] &= V(0) + L[\beta_1 S] - L[(\beta_2 + \mu)V] \\ mL[E(t)] &= E(0) + L[\alpha SI] - L[(\mu + \sigma)E] \\ mL[I(t)] &= I(0) + L[\sigma E] - L[(\mu + \delta + \rho)] \\ mL[R(t)] &= L[\rho I] - L[\mu R] \end{aligned}\right\} \qquad (28)$$

Where $S(0) = s_0, V(0) = v_0, E(0) = e_0, I(0) = i_0, R(0) = r_0$

$$\left.\begin{aligned} L[S(t)] &= \frac{s_0}{m} + \frac{\theta}{m^2} + \frac{1}{m} L[-\alpha[SI] - \beta_1 S + \beta_2 V - \mu S] \\ mL[V(t)] &= \frac{v_0}{m} + \frac{1}{m} L[\beta_1 S] - L[(\beta_2 + \mu)V] \\ mL[E(t)] &= \frac{e_0}{m} + \frac{1}{m} + L[\alpha SI] - L[(\mu + \sigma)E] \\ mL[I(t)] &= \frac{i_0}{m} + \frac{1}{m} + L[\sigma E] - L[(\mu + \delta + \rho)] \\ mL[R(t)] &= \frac{r_0}{m} + \frac{1}{m} L[\rho I] - L[\mu R] \end{aligned}\right\} \qquad (29)$$

Letting the non-linear terms $SI = A$ and substitutes by taking the inverse Laplace Transform of both sides,

$$\left.\begin{aligned} S(t) &= s_0 + \theta t + L^{-1}\left(\frac{1}{m} L[-\alpha[A] - \beta_1 S + \beta_2 V - \mu S]\right) \\ V(t) &= v_0 + L^{-1}\left(\frac{1}{m} L[\beta_1 S] - L[(\beta_2 + \mu)V]\right) \\ E(t) &= e_0 + L^{-1}\left(\frac{1}{m} + L[\alpha A] - L[(\mu + \sigma)E]\right) \\ I(t) &= i_0 + L^{-1}\left(\frac{1}{m} + L[\sigma E] - L[(\mu + \delta + \rho)]\right) \\ R(t) &= r_0 + L^{-1}\left(\frac{1}{m} L[\rho I] - L[\mu R]\right) \end{aligned}\right\} \qquad (30)$$

And the nonlinear term A is given the adomian polynomials $A_0 = S_0 I_0, A_1 = S_0 I_1 + S_1 I_0, A_2 = S_0 I_2 + S_1 I_1 + S_2 I_0,$ etc.

Thus if

$$S(t) = \sum_{k=0}^{\infty} s_n(t), V(t) = \sum_{k=0}^{\infty} v_n(t), E(t) = \sum_{k=0}^{\infty} e_n(t), I(t) = \sum_{k=0}^{\infty} i_n(t), R(t) = \sum_{k=0}^{\infty} r_n(t), \qquad (31)$$

$$\left.\begin{aligned}
\sum_{k=0}^{\infty} S_n(t) &= s_0 + \theta t + L^{-1}\left(\frac{1}{m}L\left[-\alpha\sum_{k=0}^{\infty}A_n - \beta_1\sum_{k=0}^{\infty}S_n + \beta_2\sum_{k=0}^{\infty}V_n - \mu\sum_{k=0}^{\infty}S_n\right]\right)\\
\sum_{k=0}^{\infty} V_n(t) &= v_0 + L^{-1}\left(\frac{1}{m}L\beta_1\sum_{k=0}^{\infty}S_n - L\left[(\beta_2+\mu)\sum_{k=0}^{\infty}V_n\right]\right)\\
\sum_{k=0}^{\infty} E_n(t) &= e_0 + L^{-1}\left(\frac{1}{m} + L\alpha\sum_{k=0}^{\infty}A_n - L\left[(\mu+\sigma)\right]\sum_{k=0}^{\infty}E_n\right)\\
\sum_{k=0}^{\infty} I_n(t) &= i_0 + L^{-1}\left(\frac{1}{m} + L\sigma\sum_{k=0}^{\infty}E_n - L\left[(\mu+\delta+\rho)\right]\sum_{k=0}^{\infty}I_n\right)\\
\sum_{k=0}^{\infty} R_n(t) &= r_0 + L^{-1}\left(\frac{1}{m}L\rho\sum_{k=0}^{\infty}I_n - L\mu\sum_{k=0}^{\infty}R_n\right)
\end{aligned}\right\} \quad (32)$$

The initial approximations of each class are given by;

$S_0(t) = s_0 + \theta t, V_0(t) = v_0, E_0(t) = e_0, I_0(t) = i_0, R_0(t) = r_0$ Now, comparing the coefficients $n = 1$. Using the recurrence relations, the following are obtained

For

$$S_1(t) = (\alpha i_0 s_0 - \mu s_0 - \beta_1 s_0 + \beta_1 v_0)t + \left(-\frac{1}{2}\alpha i_0\theta - \frac{1}{2}\mu\theta - \frac{1}{2}\theta\beta_1\right)t^2$$

$$V_1(t) = \left(-\mu s_0 + \beta_1 s_0 - \beta_1 v_0\right)t + \frac{1}{2}\theta\beta_1 t^2$$

$$E_1(t) = \left(\alpha i_0 s_0 - \mu e_0 - \sigma e_0\right)t + \frac{1}{2}\alpha\theta i_1 t^2 \quad (33)$$

$$I_1(t) = \left(-\delta i_0 - \mu i_0 - \rho i_0 + \sigma e_0\right)t$$

$$I_1(t) = \left(-\mu r_0 + \rho i_0\right)t$$

For n=2

$$S_2(t)=\left(\begin{array}{l}\frac{1}{2}\alpha^2 i^2 s_0+\frac{1}{2}\alpha i s_0+\frac{1}{3}\alpha i s_0\mu_0+\frac{1}{2}\alpha i s_0\rho_0-\frac{1}{2}\alpha i s_0 e_0+\frac{1}{2}\alpha i s_0\beta_1-\frac{1}{2}\alpha i s_0\beta_2\\+\frac{1}{2}\mu^2 s_0+\beta_1\mu s_0+\beta_1\mu v_0+\frac{1}{2}\beta^2 s_0+\frac{1}{2}\beta_1\beta_2 s_0-\frac{1}{2}\beta_1\beta_2 v_0-\frac{1}{2}{\beta_2}^2 v_0\end{array}\right)t^2$$

$$+\left(\frac{1}{6}\alpha^2 i^2\theta+\frac{1}{3}\alpha i_0\theta\delta+\frac{2}{3}\alpha i_0\theta\mu+\frac{1}{3}\alpha i_0\theta\rho-\frac{1}{3}\alpha e_0\theta\sigma+\frac{1}{3}\alpha i_0\theta\beta_1+\frac{1}{6}\mu^2\theta+\frac{1}{3}\beta_0\theta\mu+\frac{1}{6}{\beta_1}^2\theta+\frac{1}{6}\beta_2\theta\beta_1\right)t^3$$

$$V_2(t)=\left(-\frac{1}{2}\alpha i s_0\beta_1+\frac{1}{2}\mu^2 v_0-\beta_1\mu s_0+\beta_2\mu s_0-\frac{1}{2}\beta^2 s_0+\frac{1}{2}\beta_1\beta_2 s_0-\frac{1}{2}\beta_1\beta_2 v_0+\frac{1}{2}{\beta_2}^2 v_0\right)t^2$$

$$+\left(-\frac{1}{6}\alpha i_0\theta\beta_1-\frac{1}{3}\beta_1\mu\theta-\frac{1}{6}{\beta_1}^2\theta+\frac{1}{6}\beta_2\theta\beta_1\right)t^3$$

$$E_2(t)=\left(-\frac{1}{6}\alpha^2 i^2\theta-\frac{1}{3}\alpha i_0\theta\delta-\frac{2}{3}\alpha i_0\theta\mu-\frac{1}{3}\alpha i_0\theta\rho+\frac{1}{3}\alpha e_0\theta\sigma_1-\frac{1}{6}\mu^2\theta-\frac{1}{6}\alpha i_0\theta\beta_1\right)t^3 \quad (34)$$

$$+\left(-\frac{1}{2}\alpha^2 i^2 s_0-\frac{1}{2}\sigma i s_0-\frac{2}{3}\alpha i s_0\mu_0-\frac{1}{2}\alpha i s_0\rho_0+\frac{1}{2}\alpha i s_0 v_0-\mu^2 i e_0\beta_1+\frac{1}{2}\alpha i e_0\sigma^2\right)t^2$$

$$I_2(t)=-\frac{1}{6}\alpha^2 i^2\theta+\left(\begin{array}{l}\frac{1}{2}\sigma\alpha i s_0+\frac{1}{2}\delta^2 i_0+\delta\mu i_0-\frac{1}{2}\delta\sigma i e_0+\frac{1}{2}\mu^2 i_0-\mu\rho i_0\\-\mu\sigma i_0+\frac{1}{2}\rho^2 i_0-\frac{1}{2}\rho\sigma i e_0-\frac{1}{2}\sigma^2 e_0\end{array}\right)t^2$$

$$R_2(t)=\left(-\frac{1}{2}\delta\rho i_0+\frac{1}{2}\mu^2 r_0-\mu\sigma i_0-\frac{1}{2}\rho^2 i_0+\frac{1}{2}\rho\sigma e_0\right)t^2$$

and so on. This can be further till desired number of iterations are obtained. Thus, the obtained raw solution to each model compartment is obtained as:

$$S(t)=\sum_{k=0}^{3}s_k(t), V(t)=\sum_{k=0}^{3}v_k(t), E(t)=\sum_{k=0}^{3}e_k(t), I(t)=\sum_{k=0}^{3}i_k(t), R(t)=\sum_{k=0}^{3}r_k(t) \quad (35)$$

Evaluating these series results using the corresponding variables and parameter values,

$$S(t)=500.012-30.4440t+1.1315290300t^2--0.05075029853t^3-3.509616000\times10^{-13}t^5$$
$$-5.179149070\times10^{-7}t^4$$
$$V(t)=120-1.5060t-0.01591470000t^2+0.001033697580t^3+9.015111000\times10^{-9}t^4$$
$$E(t)=65+18.1785t-1.171778775t^2+0.04929560765t^3+5.087939775\times10^{-7}t^4+3.509616000\times10^{13}t^5 \quad (36)$$
$$I(t)=23.0.9-60t+0.0292567500t^2-0.0008440367798t^3-4.378044000\times10^{-9}t^4$$
$$R(t)=14-0.0155t-0.005054500000t^2+0.0001458242541t^3+2.473075000\times10^{-10}t^4$$

Results and Discussion

In this study, Maple 18 software was utilized to simulate the disease dynamics over time. The findings are presented in a graphical format and extensively discussed. The results presented in Figures 1, 2, and 3 provide compelling evidence of the intricate relationship between vaccination rates and the dynamics of measles transmission within the population.

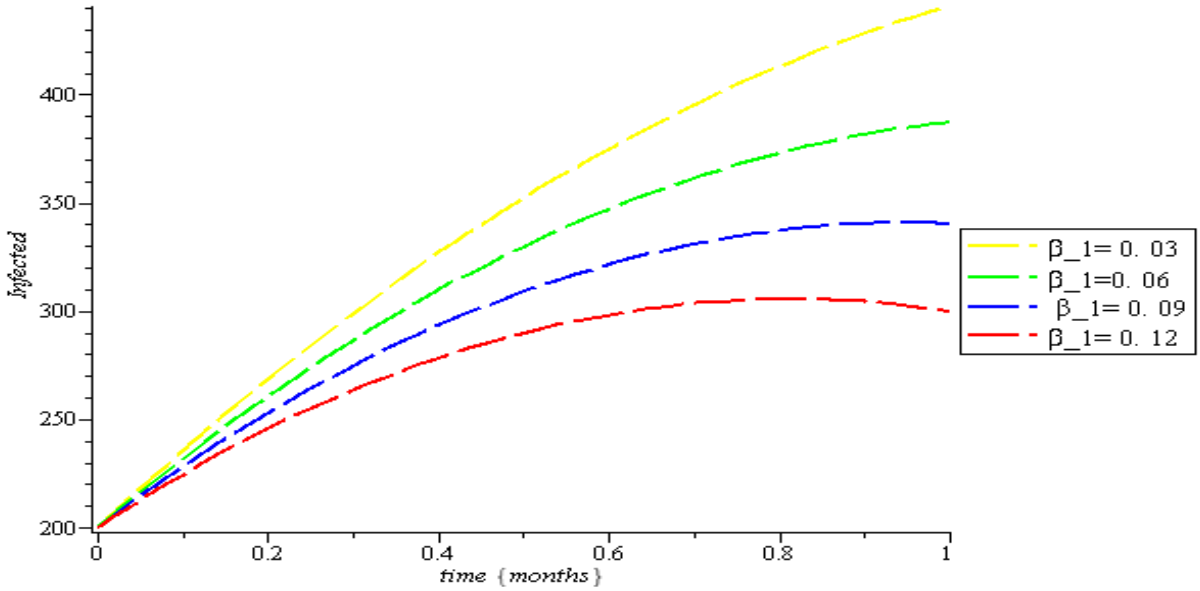

Figure 1: Effect of vaccination on infected population

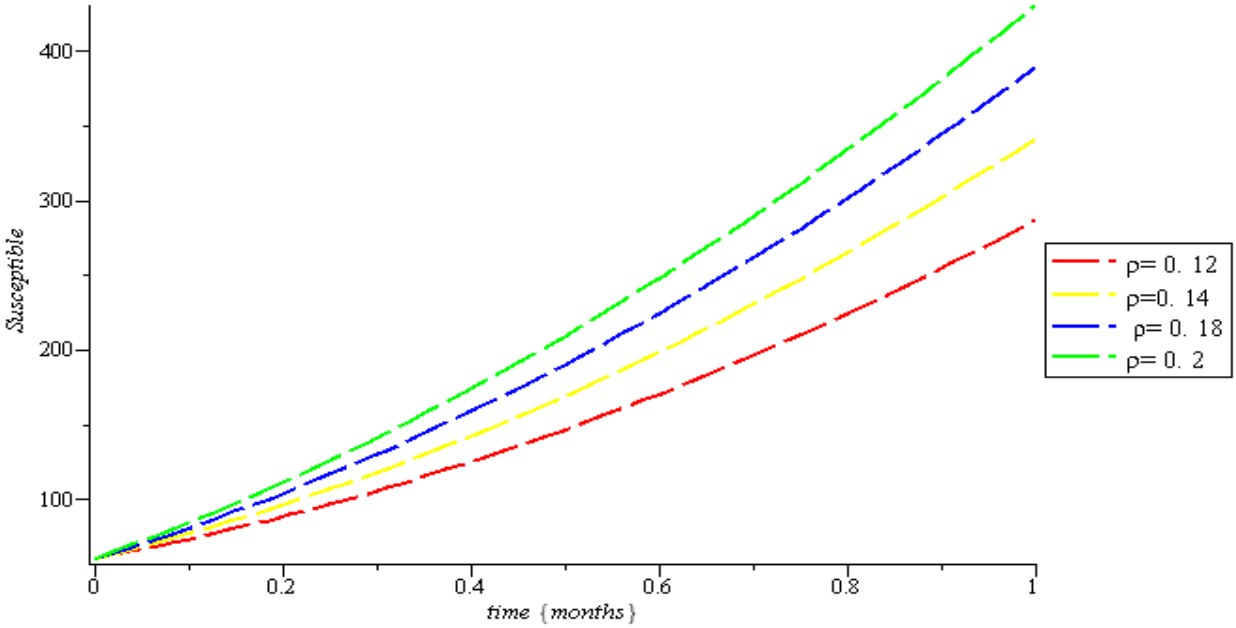

Figure 2: Rate of vaccination on susceptible population

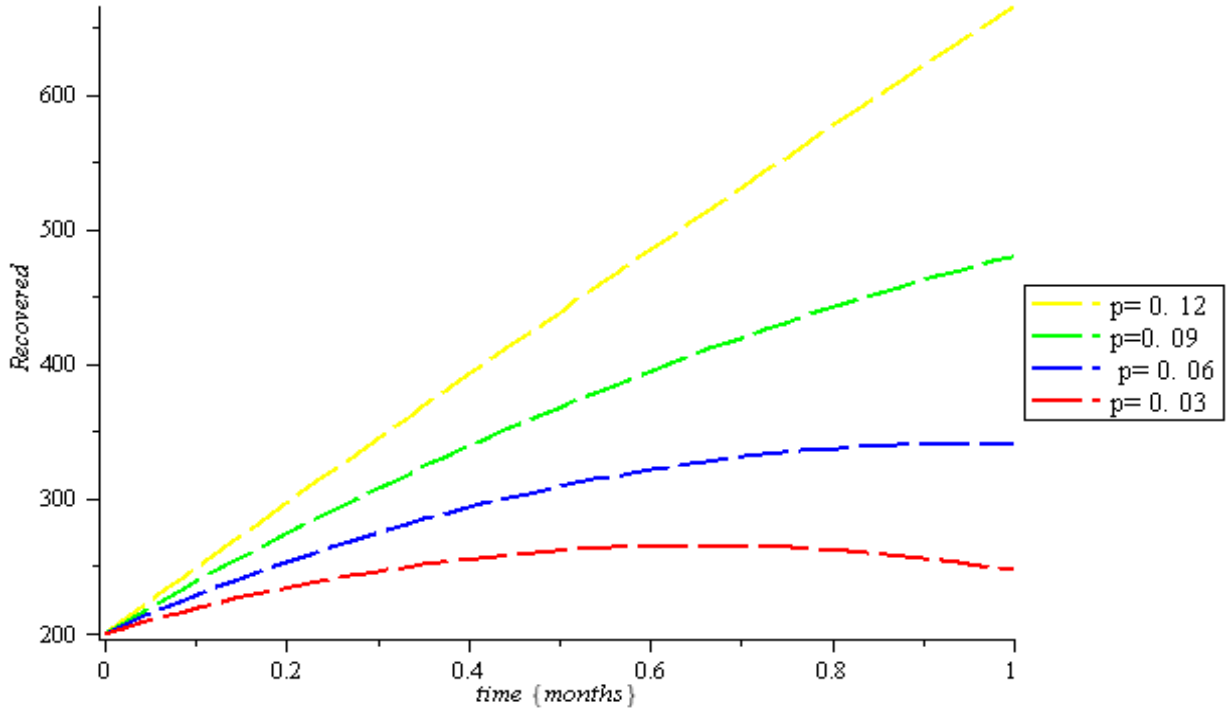

Figure 3: Effect of vaccination on individuals in recovered population

Figure 1 illustrates a clear trend: as vaccination rates increase, the number of infected individuals declines over time. This observation aligns with findings from various studies that emphasize the importance of vaccination in reducing disease incidence. For instance, effective vaccination programs have been shown to drastically lower the reproduction number (R0), ultimately leading to fewer infectionse infected population indicates the successful implementation of herd immunity, where a sufficient proportion of the population becomes immune, thus protecting even those who are unvaccinated.

In Figure 2, a nt occurs when the vaccination rate drops from 0.2 to 0.12, resulting in an increase in the susceptible population alongside a sharp decrease in the infected population. This counterintuitive finding highlights the delicate balance in disease dynamics; while lower vaccination rates may initially seem detrimental, they can lead to a temporary surge in susceptible individuals as some become exposed but not infected. This phenomenon emphasizes the need for sustained vaccination efforts to prevent resurgence of the disease. The implications of this firofound: if vaccination coverage falls below critical thresholds, even a small proportion of susceptible individuals can lead to significant outbreaks.

Figure 3 further corroborates the fiemonstrating that increased vaccination rates lead to a decrease in the exposed population. This relationship indicates that as more individuals are vaccinated, fewer are likely to contract the disease, thereby reducing the number of individuals in the exposure phase. The results underscore the importance of maintaining high vaccination coverage to minimize exposure and subsequent infection.

The observed dynamics over a one-month period when the vaccination rate is increased from 0.03 to 0.12, the number of infected individuals decreases significantly. Specifically, when the waning immunity rate is set at 0.01, the likelihood of infection diminishes, resulting in a growing population of susceptible individuals. Conversely, a reduction in the waning rate leads to an uptick in the infected population, suggesting that waning immunity is a critical factor in maintaining

disease prevalence. This highlights the necessity of booster vaccinations and ongoing public health campaigns to counteract the effects of waning immunity.

The findings from this study provide the dynamics of measles transmission and the role of vaccination. They underscore the necessity for public health initiatives aimed at increasing and maintaining vaccination rates to ensure long-term disease control and prevention. Continuous monitoring of vaccination impacts, alongside strategies to enhance public awareness and engagement, will be vital in achieving desired health outcomes and preventing future outbreaks.

Conclusion

The conclusion drawn from the graphical display of numerical results obtained through the Laplace Adomian Decomposition method underscores the critical role of vaccination in flattening epidemic curves. The method's output likely illustrates the impact of various intervention strategies on the spread of the disease. By showing how vaccination decreases the rate of infection and mitigates the severity of outbreaks, the results emphasize the importance of vaccination campaigns led by health professionals.

Vaccinating affected individuals not only reduces their susceptibility to the disease but also helps in achieving herd immunity, ultimately contributing to the stabilization and decline of epidemic curves. This conclusion highlights the urgent need for proactive vaccination efforts as a fundamental measure in controlling and containing infectious diseases.

References

Yoo, K. H., Agarwal, K., Butterfield, M., Jacobson, R. M., Poland, G. A., & Juhn, Y. J. (2018). Assessment of humoral and cell-mediated immune response to measles-mumps-rubella vaccine viruses among patients with asthma. *Allergy and Asthma Proceedings*, *31*(6), 499–506. https://doi.org/10.2500/aap.2010.31.3399

Adewale (2022). Modulating the Immune Response to Oncolytic Measles Viruses. (2022, May). *Molecular Therapy*, *9*, S108. https://doi.org/10.1016/j.ymthe.2004.06.220

Kumar, M. L., Johnson, C. E., Chui, L. W., Whitwell, J. K., Staehle, B., & Nalin, D. (2022). Immune response to measles vaccine in 6-month-old infants of measles seronegative mothers. *Vaccine*, *16*(20), 2047–2051. https://doi.org/10.1016/s0264-410x(98)00083-8

Coovadia, H., Wesley, A., Henderson, L., Brain, P., Vos, G., & Hallett, A. (2019). Alterations in Immune Responsiveness in Acute Measles and Chronic Post-Measles Chest Disease. *International Archives of Allergy and Immunology*, *56*(1), 14–23. https://doi.org/10.1159/000231998

Veklych, K. A., Popov, M. M., Liadova, T. I., & Sorokina, O. G. (2020). The Nature of a Specific Immune Response to Measles Infection of Varying Severity. *Bulletin of Problems Biology and Medicine*, *4*(1), 100. https://doi.org/10.29254/2077-4214-2020-4-158-100-104

Phillipp, J. (2020). Alterations in immune response in acute measles and chronic post-measles in chest disease Coovadia, M., Wesley, A., Henderson, G., Brain, P., Vos, G., and Hallet, F.: Int. Arch. Allergy Appl. Immunol. 56:14, 1978. *Journal of Allergy and Clinical Immunology*, *62*(4), B18. https://doi.org/10.1016/0091-6749(78)90223-3

Gans, H. A. (1998). Deficiency of the Humoral Immune Response to Measles Vaccine in Infants Immunized at Age 6 Months. *JAMA*, *280*(6), 527. https://doi.org/10.1001/jama.280.6.527

Gergonne, B. (2004). Measles outbreak casts doubt on efficacy of post-exposure measles vaccination. *Weekly Releases (1997–2007)*, *8*(8). https://doi.org/10.2807/esw.08.08.02389-en

Journal, B. S. (2014). Seroepidemiological Study of Measles Virus among Young Adults: Response to Revaccination. *Baghdad Science Journal*, *11*(4), 1493–1502. https://doi.org/10.21123/bsj.11.4.1493-1502

Measles, M. & rubella virus, v. (2015). *Reactions Weekly*, *1536*(1), 140–140. https://doi.org/10.1007/s40278-015-6992-2

Singh, H. K., Chiu, Y. L., & Wilkin, T. (2015). Measles, Mumps, and Rubella Serostatus and Response to MMR Vaccination Among HIV-Infected Adults. *AIDS Patient Care and STDs*, *29*(9), 461–464. https://doi.org/10.1089/apc.2015.0050

Griffin, D. (2016). The Immune Response in Measles: Virus Control, Clearance and Protective Immunity. *Viruses*, *8*(10), 282. https://doi.org/10.3390/v8100282

Vynnycky, E., Papadopoulos, T., & Angelis, K. (2018). The impact of Measles-Rubella vaccination on the morbidity and mortality from Congenital Rubella Syndrome in 92 countries. *Human Vaccines & Immunotherapeutics*, *15*(2), 309–316. https://doi.org/10.1080/21645515.2018.1532257

Oh, C., Rafai, E., Cho, Y., Jun, D., & Cha, S. (2022). An Economic Analysis of Mumps Vaccination in Fiji: Static Model Simulation of Routine Measles–Mumps–Rubella (MMR) Vaccination Instead of Current Measles–Rubella (MR) Vaccination. *International Journal of Environmental Research and Public Health*, *19*(3), 2020. https://doi.org/10.3390/ijerph19031861

Suwoyo, S., Yani, E. R., & Hardjito, K. (2023). COVID-19 immune response in adults post Measles-Rubella vaccination. *Vacunas*, *24*(4), 341–347. https://doi.org/10.1016/j.vacun.2023.05.004

Berhe, H. W., & Makinde, O. D. (2020). Computational modelling and optimal control of measles epidemic in human population. *Biosystems*, *190*, 104102. https://doi.org/10.1016/j.biosystems.2020.104102

Berkovich, S., & Starr, S. (1964). Use of live-measles-virus vaccine to abort an expected outbreak of measles within a closed population. *Nursing Research*, *13*(2), 178. https://doi.org/10.1097/00006199-196401320-00035

James, J. J., Halvorson, G. W., Gates, J. R., & Oo, C. T. (1979). Measles-like Disease and Measles Antibody Titers in an Adult Population. *Military Medicine*, *144*(10), 672–676. https://doi.org/10.1093/milmed/144.10.672

Kulsoom, S., Soomro, S., Junejo, S., Anjum, M., Waseem, H., & Akram, M. (2023). Clinical Presentation, Complications and Outcome of Measles in Pediatric Population at Tertiary Care Hospital. *Pakistan Journal of Health Sciences*, 50–53. https://doi.org/10.54393/pjhs.v4i03.624

Palumbo, P., Hoyt, L., Demasio, K., Oleske, J., & Connor, E. (1992). Population-based study of measles and measles immunization in human immunodeficiency virusinfected children. *The Pediatric Infectious Disease Journal*, *11*(12), 1008–1014. https://doi.org/10.1097/00006454-199211120-00004

Plans-Rubió, P. (2020). Are the Objectives Proposed by the WHO for Routine Measles Vaccination Coverage and Population Measles Immunity Sufficient to Achieve Measles Elimination from Europe? *Vaccines*, *8*(2), 218. https://doi.org/10.3390/vaccines8020218

Wang, Z., Yan, R., He, H., Li, Q., Chen, G., Yang, S., & Chen, E. (2014). Difficulties in Eliminating Measles and Controlling Rubella and Mumps: A Cross-Sectional Study of a First Measles and Rubella Vaccination and a Second Measles, Mumps, and Rubella Vaccination. *PLoS ONE*, *9*(2), e89361. https://doi.org/10.1371/journal.pone.0089361

How to cite this paper:
Alade, F.A., Alabi, P.A., Ankeli, U.C., Mubarak, S. (2024). On the Laplace Adomian Decomposition Method Numerical Analysis of the Vaccine's Effect on Measles. *Malaysian Journal of Applied Sciences,* 9*(*2), 77-95.